# Characterization of bacterial cellulose films combined with chitosan and polyvinyl alcohol: Evaluation of mechanical and barrier properties

Patricia Cazón[1,2], Gonzalo Velázquez[1*], Manuel Vázquez[2*]

[1]Instituto Politécnico Nacional. CICATA unidad Querétaro. Cerro Blanco No. 141. Colinas del Cimatario, Querétaro, 76090, México.

[2]Department of Analytical Chemistry, Faculty of Veterinary, University of Santiago de Compostela, 27002-Lugo, Spain

*Corresponding author: manuel.vazquez@usc.es

gvelazquezd@ipn.mx; phone +52 (442)-229-0804 Ext 81058.

## Abstract

Bacterial cellulose (BC) produced by *Komagataeibacter xylinus* is a biomaterial with a unique three-dimensional structure. To improve the mechanical properties and reinforce the BC films, they were immersed in polyvinyl alcohol (0-4%) and chitosan (0-1%) bathes. Moisture content, mechanical properties and water vapour permeability were measured to assess the effect of polyvinyl alcohol and chitosan. The morphology, optical, structural and thermal properties were evaluated by scanning electron microscopy, spectral analysis, thermogravimetry and differential scanning calorimetry. Results showed that moisture content was significantly affected by the chitosan presence. Tensile strength values in the 20.76 - 41.65 MPa range were similar to those of synthetic polymer films. Percentage of elongation ranged from 2.28 to 21.82% and Young's modulus ranged from 1043.88 to 2247.82 MPa. The water vapour permeability

(1.47·$10^{-11}$ - 3.40·$10^{-11}$ g/m·s·Pa) decreased with the addition of polyvinyl alcohol. The developed films own UV light barrier properties and optimal visual appearance.

**Keywords:** Films; bacterial cellulose; water vapor permeability; chitosan; polyvinyl alcohol; UV protection.

## 1. Introduction

In the last decade, research in biopolymers has been widely carried out to design and develop renewable, biodegradable and biocompatible products with applications in medicine, pharmacy, cosmetics, food industry and biotechnology (Hu, Chen, Yang, Li, & Wang, 2014). Among biopolymers, cellulose is the most abundant natural compound on the earth. This low-cost biopolymer has renewability, non-toxicity, biocompatibility, biodegradability and chemical stability (Cazón, Velazquez, Ramírez, & Vázquez, 2017). Due to the properties of cellulose, it has become a very interesting material to develop new biodegradable polymers, like biofilms aimed to food packaging applications.

Cellulose is a highly crystalline polymer formed by a linear chain with two anhydroglucose rings (($C_6H_{10}O_5)_n$), covalently linked through an oxygen in a β(1-4) glycosidic bond. Cellulose possesses abundant hydroxyl groups forming plenty inter- and intra-molecular hydrogen bonds (Cazón et al., 2017). It is found in plant cell wall and accordingly, it can be obtained from wood, cotton, hemp and plant-based materials. Furthermore, cellulose is also produced by tunicates, several species of algae, and by some species of bacteria including *Acetobacter*, *Agrobacterium*, *Pseudomonas*,

*Rhizobium*, *Sarcina and Komagataeibacter xylinus.* The last one was renamed as *Acetobacter xylinum* and more widespread as *Gluconoacetobacter xylinus* (Szymańska-Chargot et al., 2017; Yamada et al., 2012). It produces high amounts of cellulose, being one of the most commonly studied sources of bacterial cellulose (BC) (Mohammadkazemi, Azin, & Ashori, 2015; Ruka, Simon, & Dean, 2012).

In a suitable culture medium and static conditions, *G. xylinus* synthesizes BC in the form of pellicle on the surface of the liquid medium. This microorganism produces glucose chains from the carbon source contained in the medium. The glucose chains are extruded out through tiny pores present on their cell wall. Combining the glucose chains, the microorganism forms microfibrils that aggregate to form cellulose ribbons. These ribbons form a three-dimensional structure consisting of an ultrafine network of cellulose nanofibers with an expanded surface area and high porosity. The three-dimensional structure determines its physical and mechanical properties (Jozala et al., 2016; Shah, Ul-Islam, Khattak, & Park, 2013; Shao et al., 2016). Unlike vegetable cellulose, BC is obtained with high purity, free of vegetable remains such as lignin and hemicellulose (Jozala et al., 2016).

Several studies have been focused on developing new films based on BC. Usually, BC films are combined with other polymers or plasticizers to improve or modify the physicochemical properties and expand its potential applications. There are two main strategies to combine BC with other polymers or plasticizers, keeping the film structure obtained from the fermentation process. One option is by supplementation the culture medium with the desirable reinforcing agents, such as *Aloe vera* (Saibuatong & Phisalaphong, 2010a), chitosan (Phisalaphong & Jatupaiboon, 2008), polyvinyl alcohol

(PVOH) (Gea, Bilotti, Reynolds, Soykeabkeaw, & Peijs, 2010) or polyethylene oxide (Brown & Laborie, 2007). Other strategy is by immersion of the BC film in a bath with a solution of the desirable polymer or plasticizer, e.g. polyvinyl alcohol (PVOH) (Gea et al., 2010), polyethylene glycol or diacrylate (Cai & Kim, 2010; Numata, Sakata, Furukawa, & Tajima, 2015).

A widespread practice is to use nanofibers or nanowhiskers of BC as reinforcing agent. BC pellicles are usually subjected to a hydrolysis process using strong acids, breaking down the structure of the material into nanofibers or nanocrystals (Martínez-Sanz, Lopez-Rubio, & Lagaron, 2013). These BC nanocomponents are incorporated into the matrix of a polymer to modify the properties of the composite film such as starch (Martins et al., 2009), PVOH (Jipa et al., 2012), arabinogalactan and xyloglucan (Lucyszyn et al., 2016), chitosan (Salari, Sowti Khiabani, Rezaei Mokarram, Ghanbarzadeh, & Samadi Kafil, 2018; Velásquez-Cock et al., 2014; Wang, Xie, et al., 2018), polylactic acid, polyethylene glycol (Martínez-Sanz et al., 2013), fish proteins (Shabanpour, Kazemi, Ojagh, & Pourashouri, 2018), gelatin (George & Siddaramaiah, 2012) or agar (Wang, Guo, et al., 2018) among other biopolymers.

From the strategies mentioned to obtain BC-polymers composite films, it is interesting to pay special attention to the immersion method. It is a simple technique that allows using the films formed from the culture medium. This method allows avoiding previous steps of dissolution, regeneration or homogeneous dispersion of the cellulose, simplifying the process. In addition, this technique allows taking advantage of the unique structure of the BC as the main component of the final matrix. On the other hand, unlike the supplementation culture media method, by immersion allows

93 expanding the range and concentration of the possible combinations. Some
94 supplementation components in the culture media can interfere with the cellulose
95 production yield. Hence, the concentration of these components in the formulation film
96 are limited (Phisalaphong & Jatupaiboon, 2008; Saibuatong & Phisalaphong, 2010a).

97 Following the strategy of combining polymers to improve the properties of the
98 final material, PVOH and chitosan can improve the potential applications of BC-based
99 films. PVOH is a hydrophilic semi-crystalline polymer produced by polymerization of
100 vinyl acetate to polyvinyl acetate, followed by a hydrolysis process. It is a synthetic
101 polymer, water soluble, non-toxic, biodegradable, with film forming properties, optimal
102 transparency and good elasticity properties (Carvalho et al., 2009; Cazón, Vázquez, &
103 Velazquez, 2018a). These properties make PVOH an ideal polymer to combine with BC
104 by immersion.

105 Chitosan is one of the most studied polysaccharides with potential applications
106 in biomedical, food, and chemical industries. It is the second most abundant
107 polysaccharide in nature. It can be obtained mainly from residues of the shellfish
108 industry. This polymer is non-toxic, biodegradable, with film forming properties and
109 soluble in dilute organic acids such as acetic acid. One of the most interesting properties
110 of the chitosan is its antimicrobial activity against a wide range of foodborne
111 filamentous fungi, yeast, and bacteria, being more active against yeasts (Helander,
112 Nurmiaho-Lassila, Ahvenainen, Rhoades, & Roller, 2001; No, Meyers, Prinyawiwatkul,
113 & Xu, 2007). Among these properties, its solubility and antimicrobial activity make it
114 an ideal polymer to combine with BC by immersion. Incorporating antimicrobial agents
115 from natural source into BC composite films addresses the current consumer demand of

a natural alternative to chemically synthesized antimicrobial polymers. In food packaging, a strategy to increase the shelf life is to develop active films with antimicrobial properties. The direct contact with the active films inhibit the growth of microorganisms on the surface of the food (Broek Van Den, Knoop, Kappen, & Boeriu, 2015; Moreira, Roura, & Ponce, 2011).

In previous studies of our group, films based on regenerated vegetable cellulose-PVOH-chitosan were characterized. The results obtained suggested an adequate interaction of cellulose-chitosan-PVOH to combine both polymers by immersion, improving the film properties (Cazón, Vázquez, & Velazquez, 2018b; Cazón et al., 2018a). Nevertheless, as mentioned, there are important structural differences between vegetable cellulose and BC. These differences could affect the interactions of cellulose-PVOH-chitosan, improving the properties of the cellulose-based films and expanding its potential applications. Besides, it was observed the low transmittance of regenerated cellulose and chitosan films developed, manifested UV protect properties of cellulose-based films (Cazón et al., 2018a). Packaging materials against UV light has received a great deal of attention since UV-light is one of those responsible factors of the oxidative process in vitamins, lipids and proteins. These oxidative process produce undesirable off-flavours that decrease the shelf-life of the products (Olarte, Sanz, Federico Echávarri, & Ayala, 2009). Hence, the UV-barrier properties observed increase the interest in the development of BC-based films for food applications.

On the other hand, the application of BC-PVOH-chitosan components in the field of controlled drug administration has been also studied. The results suggested that BC-PVOH-chitosan composites could be used as a biopolymeric carrier for drug

delivery applications (Pavaloiu, Dobre, & Hlevca, 2013). Despite the good interaction among these biodegradable polymers, the characterization of these films has not been carried out to aim applications like biopolymers for active food packaging.

The aim of this work was to developed biodegradable films based on BC with chitosan and PVOH to enhance the mechanical and optical properties to obtain cellulose films more manageable and transparent with antimicrobial and UV-barrier properties. The effect of the ratio of these polymers incorporated to the BC matrix by immersion, maintaining intact the characteristic BC structure, was studied and compared to regenerated cellulose, previously analysed. Polynomial models were used to evaluate the effect of the composition of the blend on the moisture content, mechanical properties (tensile strength, percentage of elongation to break and Young's Modulus) and water vapour permeability. Besides, microstructure, optical properties, structure and thermal analyses of the BC-PVOH-chitosan films were also evaluated.

## 2. Materials and methods

*Komagateibacter xylinus* was obtained from the "Colección Española de Cultivos Tipo" (CECT, Valencia, Spain). Extra pure anhydrous sodium bromide (99 %), sodium hydroxide (98 %) and D(+)-glucose monohydrate (99% extra pure) were purchased from Acros organics (Geel, Belgium). Yeast extract was provided by Scharlau Microbiology (Barcelona, Spain). Full-hydrolyzed (>98%) polyvinyl alcohol with average molecular weight (Mw) of 30,000 g/mol and ester value of 12-25 were supplied by Merck (Billerica, MA, US). Chitosan (Mw 100000-300000) was purchased from Acros organics (Geel, Belgium).

### *2.1. Preparation of bacterial cellulose films*

The preparation process is shown in Figure 1. Initial culture medium was prepared from 10% of glucose and 1% of yeast extract and sterilized at 121ºC for 15 min. A pre-culture was prepared by transferring 5 mL of a stock culture to 300 mL of medium in a Petri dish and incubated statically at 30 ºC for 2 days. Then, Petri dishes were prepared with 75 ml of culture medium and inoculated with 5 ml of the pre-culture. Petri dish was stored at 30 ºC for 8 days. After that time, the film was suspended in the air-liquid medium. The films were treated with 1% (w/v) of NaOH at 90 ºC for 1 h to remove bacterial cells and washed with running distillate water until pH 7. Finally, BC films were dried at room temperature for 48 h.

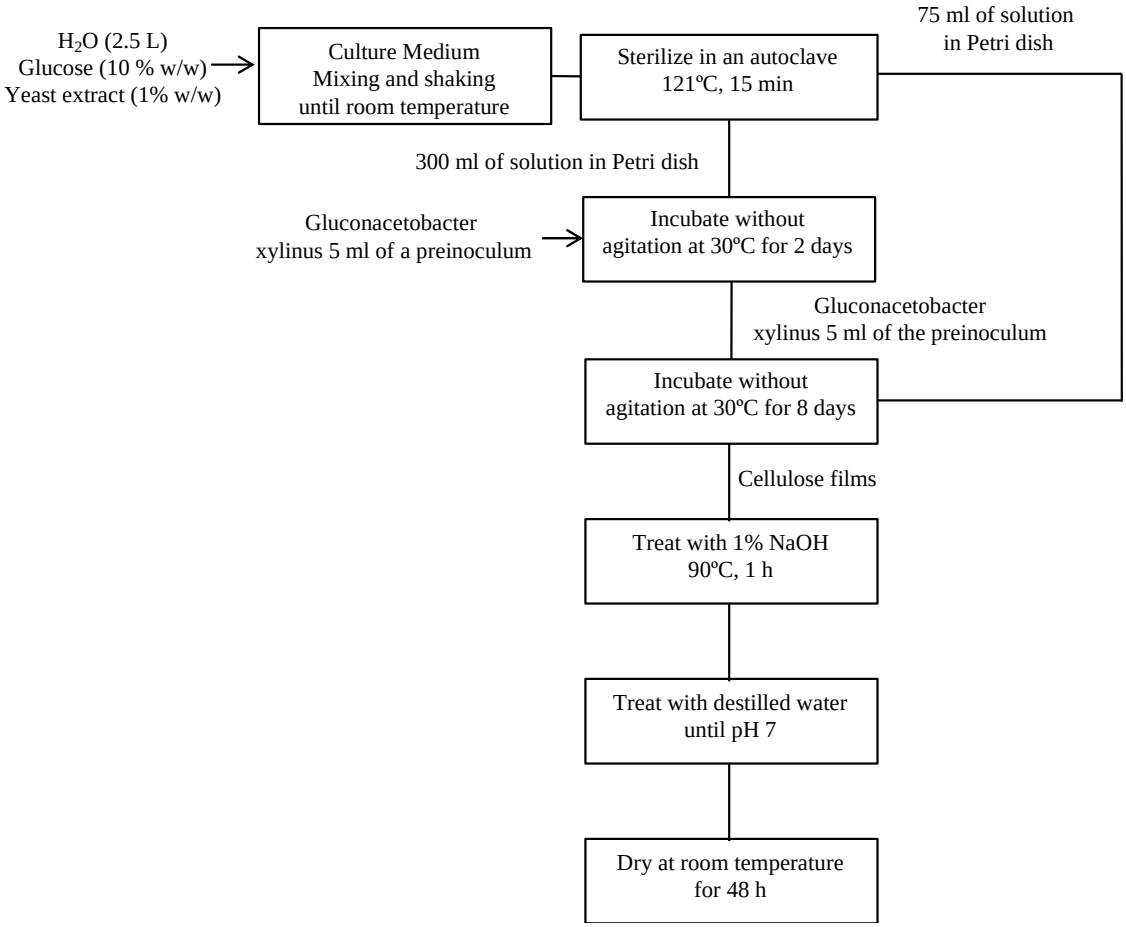


Fig. 1. Overall process proposed for the production of bacterial cellulose-based films.

### *2.2. Preparation of bacterial cellulose-chitosan-PVOH composite films*

The resulting wet bacterial films were placed between two sheets of filter paper to remove excessive water. Then, films were immersed in a bath of the mixture chitosan-PVOH. The solution of chitosan was prepared from an aqueous solution of 1% (v/v) of acetic acid at room temperature with vigorous agitation. The PVOH solution was prepared from an aqueous solution heated at 80 ºC with vigorous agitation for 2 h. Finally, the BC-PVOH-chitosan films were dried in a Petri dish at room temperature for

2 days. The dried films were cut to specific sizes for each test. The samples were stored in desiccators with saturated salt of sodium bromide or silica gel for 5 days as required for each test.

### *2.3. Film thickness measurement*

Films thickness (mm) was measured using a thickness meter ET115S (Etari GmbH, Stuttgart, Germany). The measuring was carried out at 5 locations prior to the characterization tests. The average thickness of the films for each formulation are shown in Table 1.

### *2.4. Scanning electron microscopy (SEM)*

Films were fixed on slides with adhesive carbon tape, metalized with Au, observed and photographed with a high-vacuum microscope (JEOL JSM-6360LV, Jeol Ltd, Tokyo, Japan) at an accelerating voltage of 20 kV.

### *2.5. Moisture content at equilibrium*

The water content of the samples stored in desiccators with saturated salt of sodium bromide for 5 days was determined measuring the weight loss. Film portions of 3×3 $cm^2$ stored in a desiccator with saturated sodium bromide solution were weighed to the nearest 0.0001 g for the initial sample weight. Then, the samples were dried at 105 ˚C in a vacuum oven for 24 h until constant weight (dry sample weight). Samples were analyzed by triplicate. Equilibrium moisture content (%) was calculated using the Equation (1):

$$\text{Equilibrium moisture content (\%)} = \frac{\text{Initial weight} - \text{Dry weight}}{\text{Initial weight}} \times 100 \quad \text{(Eq. 1)}$$

### *2.6. Water vapour permeability*

Water vapor permeability (WVP) quantifies the amount of water that diffuses through the film per unit area and time (g/s·m·Pa), depending on the differential pressure and film thickness. WVP values were obtained gravimetrically following the ASTM Standard Test Method E96 (https://www.astm.org/Standards/E96.htm). A wide-mouth cup ($5 \cdot 10^{-3}$ $m^2$ area) containing 100 ml of distilled water was sealed with the select films. The cup was placed in the centre of a double-bottom box containing silica gel and placed on the plate of a precision balance. The gradient of partial pressure between both sides of the film produced a driving force for the water flux trough the film. The water flux resulted in a decrease of the weight of the cup. Tests were run at 30 ºC for at least 8 h that it is enough time to reach the equilibrium of the water flux. Weight loss of the cup was recorded to the nearest $1 \cdot 10^{-4}$ g and plotted as a function of time (Gennadios, Weller, & Gooding, 1994). The slope was evaluated by linear regression ($r^2$>0.99). WVP was calculated according to the combined Fick and Henry laws for gas diffusion through films, using the Equation 2.

$$WVP = \frac{\Delta w \cdot x}{\Delta t \cdot A \cdot \Delta P} \quad \text{(Eq. 2)}$$

Where $\Delta w/\Delta t$ *(g/s)* is the flux measured as weight loss of the cell per unit of time, *x (m)* is the film thickness, *A* ($m^2$) is the exposed area and $\Delta P$ (Pa) is the water vapour pressure differential calculated as 4245 Pa at 30 ºC (Wexler, 1976). Each test was performed in triplicate.

*2.7. Mechanical properties*

The mechanical properties were measured using a texturometer (TA-XTplus, Stable Micro System, UK). Tensile strength (TS, the maximum stress before breaking), percentage of elongation at break (%E, the maximum elongation of the film before rupture) and Young's Modulus (YM, yield stress divided by yield strain in the viscoelastic region) were measured following the standard method D-882 (ASTM). The tests were run with an initial grip separation of 40 mm and a crosshead speed of 0.08 mm/s. Ten samples of each formulation were previously cut into 15×100 mm samples and stored in desiccators with saturated salt of sodium bromide for 5 days. Both ends of the films were fixed in the grips and the strength during extension was measured.

In each test, TS and %E were calculated using the Equations 3 and Equation 4, respectively (Antoniou, Liu, Majeed, & Zhong, 2015):

$$TS\ (MPa) = \frac{F}{L \cdot x} \qquad \text{(Eq. 3)}$$

$$\%E\ (\%) = \frac{l - l1}{l1} \cdot 100 \qquad \text{(Eq. 4)}$$

In the Equation 3, $F$ is the maximum force before breaking (N), $L$ is the width of the film (mm) and $x$ is the thickness (mm). In the Equation 4, $l_1$ is the initial length (mm) and $l$ is the length of the film (mm) at the breaking point. Young's modulus was calculated from the slope of the curve stress-strain curve in the viscoelastic region.

### *2.8. Light barrier properties, transparency and opacity*

A spectrophotometer V-670 (Jasco Inc, Japan) was used to analyze the ultraviolet and visible light barrier properties of the film, using transmittance mode at 2 nm intervals in UV-VIS-NIR regions (190 nm–2500 nm). The test was done in duplicate for each sample. The transparency of the films was calculated from the percent of transmittance at 600 nm using the Equation 5 (Han & Floros, 1997).

$$Transparency = \frac{(\log \%T_{600})}{x} \quad \text{(Eq. 5)}$$

Where $\%T_{600}$ is the percent transmittance at 600 nm and $x$ is the film thickness (mm). The opacity of the films was calculated from de absorbance of light at 500 nm, following the Equation 6 (Kanatt, Rao, Chawla, & Sharma, 2012).

$$Opacity = \frac{Abs_{500}}{x} \quad \text{(Eq. 6)}$$

Where $Abs_{500}$ is the absorbance at 500 nm and $x$ is the film thickness (mm).

### 2.9. *Fourier transform infrared spectroscopy (FT-IR)*

A FT-IR (Bomen 102. ABB Ltd, Zurich Switzerland) equipped with a Universal Attenuated Total Reflectance (UATR) accessory with diamond crystal was used to collect the FT-IR spectra of the films. Samples were conditioned at relative humidity of 65±2% and 21±1°C for at least 48 h prior to the test. FT-IR spectra were collected at a spectral resolution of 4 $cm^{-1}$ over the range from 400 to 4000 $cm^{-1}$.

### 2.10. *Thermal properties of films*

The thermal stability of the developed films was analyzed using a Thermogravimetric Analyzer/Differential Scanning Calorimeter (TGA/DSC1) equipment (Mettler-Toledo International Inc., Columbus, OH). The samples (around 2-4 mg ) were placed in hermetic aluminum pans and the test was carried out at a heating rate of 10°C/min from 50 to 400°C, in atmosphere of $N_2$ (50 mL/min).

### 2.11. *Statistical analysis*

PVOH and chitosan concentration were considered as independent variables (denoted A and B, respectively) and the effect on the select dependent variables (moisture content, TS, %E, YM and VWP) were calculated. The set of experiments followed a factorial design. Table 1 shows the experiment design. Cook's distance was used the detect outliers (Cook, 1977) and the Box-Cox data transformation was used to reduce anomalies (Sakia, 1992). The multifactor analysis of variance (ANOVA) was used. The statistical analysis was accomplished using Design Expert ® 10.0.6 software (Stat-Ease, Inc., Minneapolis, MN, USA).

Table 1. Formulations assayed for the study of bacterial cellulose based films combined with chitosan and polyvinyl alcohol and experimental results for the mechanical and permeability properties of the films achieved. MC is the equilibrium moisture content of each sample after being stored in desiccators with saturated salt of sodium bromide for 5 days, TS is tensile strength, %E is percentage of elongation at break, YM is Young's modulus and WVP is water vapour permeability.

| Exp. | Chitosan % (w/w) | PVOH % (w/w) | Thickness mm | MC % | TS MPa | %E % | YM MPa | WVP g/m s Pa |
|---|---|---|---|---|---|---|---|---|
| 1 | 0 | 0 | $2.08 \cdot 10^{-2}$ | 1.82 | 20.76 | 2.28 | 1043.88 | $2.38 \cdot 10^{-11}$ |
| 2 | 0 | 2 | $5.07 \cdot 10^{-2}$ | 8.58 | 30.59 | 4.60 | 1595.16 | $1.47 \cdot 10^{-11}$ |
| 3 | 0 | 4 | $6.62 \cdot 10^{-2}$ | 8.06 | 27.50 | 9.99 | 1055.57 | $1.85 \cdot 10^{-11}$ |
| 4 | 0.5 | 0 | $2.36 \cdot 10^{-2}$ | 6.41 | 33.37 | 4.60 | 1443.45 | $2.46 \cdot 10^{-11}$ |
| 5 | 0.5 | 2 | $3.98 \cdot 10^{-2}$ | 8.73 | 38.89 | 4.71 | 2247.82 | $2.06 \cdot 10^{-11}$ |
| 6 | 0.5 | 4 | $5.04 \cdot 10^{-2}$ | 8.46 | 38.29 | 5.57 | 1825.22 | $2.21 \cdot 10^{-11}$ |
| 7 | 1 | 0 | $2.99 \cdot 10^{-2}$ | 12.55 | 39.28 | 7.08 | 1579.59 | $2.79 \cdot 10^{-11}$ |
| 8 | 1 | 2 | $5.17 \cdot 10^{-2}$ | 10.68 | 41.65 | 13.20 | 1363.63 | $2.68 \cdot 10^{-11}$ |
| 9 | 1 | 4 | $5.71 \cdot 10^{-2}$ | 9.89 | 36.81 | 21.82 | 1174.37 | $3.40 \cdot 10^{-11}$ |

## 3. Results and discussion

Biodegradable films were obtained using bacterial cellulose, PVOH and chitosan at several concentrations following the experimental design showed in Table 1. The concentration of PVOH in the bath ranged from 0 to 4% (w/w) and chitosan ranged

from 0 to 1% (w/w). At higher concentrations of chitosan and PVOH, the bath was very viscous resulting in too thick films. The average thickness of the films and the results obtained for dependent variables (moisture content, TS, %E, YM and WVP) are listed in Table 1. The effect of the PVOH and chitosan on the dependent variables (moisture content, TS, %E, YM and WVP) were modelled using a second-order polynomial equation. The ANOVA results of the dependent variables are shown in Table 2. Table 2 also shows the fit statistics values of $r^2$, predicted $r^2$, adjusted $r^2$ and adequate precision for each dependent variable analyzed.

Table 2. Analysis of variance (ANOVA) for each of the study dependent variables. TS is tensile strength, %E is percentage of elongation at break, YM is Young's modulus, WVP is water vapour permeability, MC is the equilibrium moisture content of each sample after being stored in desiccators with saturated salt of sodium bromide for 5 days.

| | MC | | TS | | %E | | YM | | WVP | |
|---|---|---|---|---|---|---|---|---|---|---|
| Source | F-value | p-value | F-value | p-value | F-value | p-value | F-value | p-value | F-value | p-value |
| Model | 9.04 | 0.0184 | 30.63 | 0.0089 | 9.80 | 0.0129 | 302.83 | 0.0033 | 20.11 | 0.0163 |
| A-Chitosan | 15.96 | 0.0104 | 107.55 | 0.0019 | 10.39 | 0.0181 | 63.87 | 0.0153 | 68.39 | 0.0037 |
| B-PVOH | 2.35 | 0.1862 | 5.98 | 0.0920 | 9.21 | 0.0230 | 153.05 | 0.0065 | 0.19 | 0.6905 |
| AB | 8.81 | 0.0312 | 9.05 | 0.0573 | | | 79.11 | 0.0124 | 13.08 | 0.0363 |
| $A^2$ | | | 14.23 | 0.0326 | | | 1054.5 | 0.0009 | 2.78 | 0.1942 |
| $B^2$ | | | 16.35 | 0.0272 | | | 655.51 | 0.0015 | 16.13 | 0.0277 |

| | | | | | |
|---|---|---|---|---|---|
| $r^2$ | 0.98 | 0.98 | 0.77 | 0.99 | 0.99 |
| Adjusted $r^2$ | 0.97 | 0.95 | 0.69 | 0.99 | 0.99 |
| Predicted $r^2$ | 0.95 | 0.79 | 0.45 | 0.98 | 0.95 |
| Adequate precision | 25.55 | 16.94 | 8.85 | 48.82 | 39.39 |

### *3.1. Scanning electron microscopy (SEM)*

The top and bottom surfaces of both sides and cross section of the films obtained in experiments 1, 3 and 7 were observed by scanning electron microscopy (SEM). Figure 2 shows the top and bottom surface of the films as well as the cross section. The selected experiments allowed to analyse the effect of the PVOH and chitosan on the microstructure of the bacterial cellulose films. As shown Figure 2a, bacterial cellulose films presented a continuous matrix with a porous surface. Bottom side showed a denser surface and a rough layer on the opposite side. The difference between both sides depended on the fermentation process. Probably, the less dense and porous side was the most recently formed. The cross section of the bacterial cellulose films (Figure 2a) showed a laminated structure. The acetic bacteria form the pellicle layer by layer. In general, the addition of PVOH and chitosan resulted in a softening of the surface, decreasing the roughness and porosity (Figure 2b and 2c). The bottom sides were smoother than the top because they were in contact with the Petri dish during the drying. According to the cross-section micrographs of the experiment 3 (Figure 2b) and 7 (Figure 2c), PVOH and chitosan increased the thickness and the density of the film promoting a more compact structure. The thickness increase was more important in formulations containing PVOH than those with chitosan. Chitosan and PVOH had a

329 similar effect on the surface and on the microstructure than that on vegetable
330 regenerated cellulose films studied in previous work (Cazón et al., 2018b, 2018a).

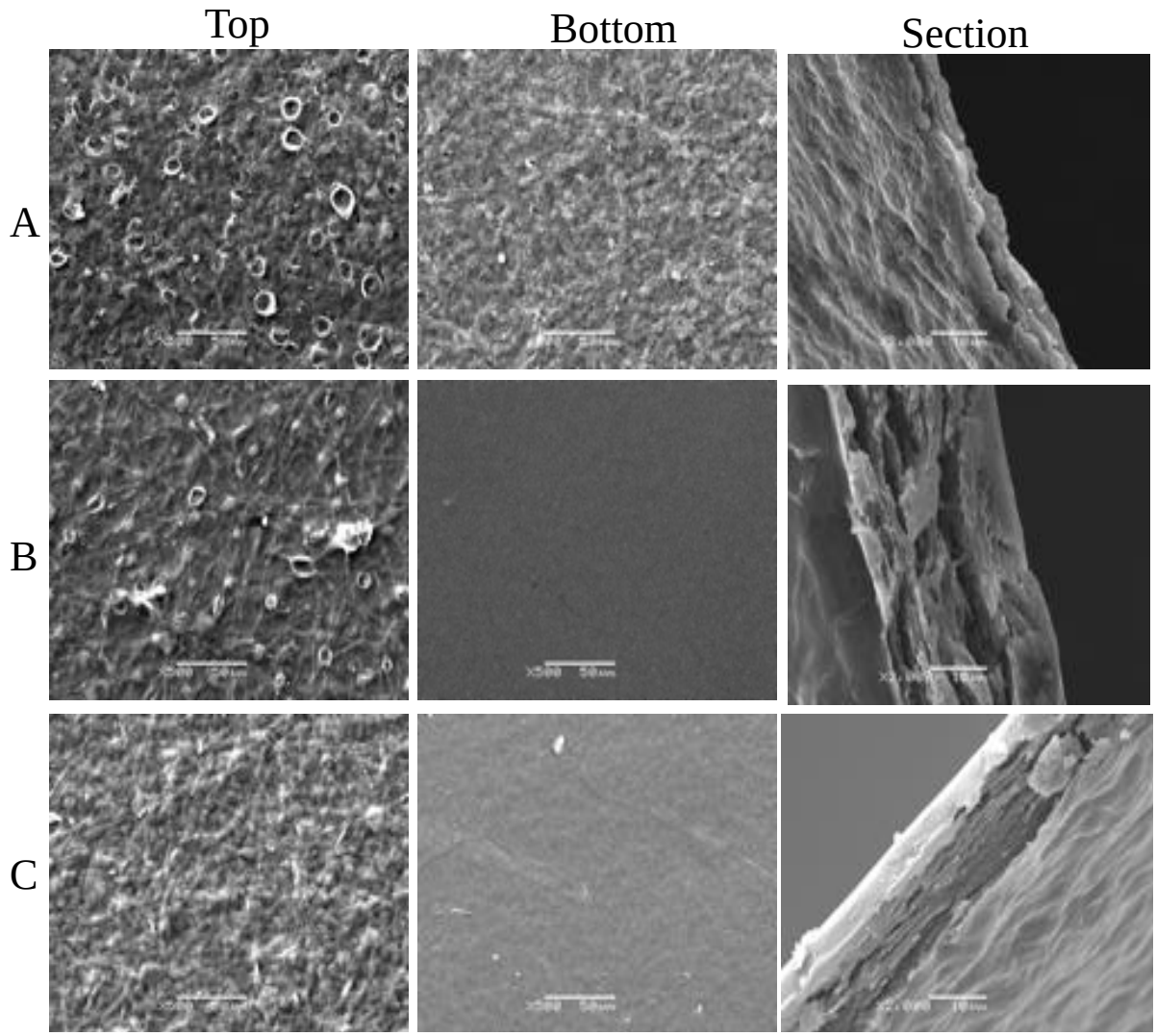


331

332

333 Fig. 2. Scanning electron microscopy of the samples as well of the section of the films
334 of experiments 1, 3 and 7. A) Pure bacterial cellulose sample. B) Bacterial cellulose-
335 poly(vinyl alcohol) 4% (w/w). C) Bacterial cellulose-chitosan 1% (w/w).

336

### *3.2. Moisture content at equilibrium*

The content of the moisture of the samples were analysed. Bacterial cellulose, chitosan and PVOH are hydrophilic components, but with different affinity and interaction capacity with water. The moisture content can modify the properties of the films, mainly the mechanical properties. Hence, determining the moisture content of each formulation can help to interpret the other tests. The moisture content of the developed films conditioned in desiccators with saturated sodium bromide solution for 5 days ranged from 1.82 to 12.55%. Data fitted well to a two-factor interaction mathematical model. The trial 2 was ignored for ANOVA analysis as it was detected as an outlier in the Cook's distance test. The F-value of the model was 68.85 indicating that the model was significant. The p-values of the model terms were significant ($p < 0.05$). The $r^2$ value was 0.98. Adjusted $r^2$ compares the goodness-of-fit for regression models that contain differing numbers of independent variables. Predicted $r^2$ is a measure of how well the model predicts a response value. The adjusted $r^2$ and predicted $r^2$ should be within approximately 0.20 of each other to be in reasonable agreement. In this case, the difference between the predicted $r^2$ (0.98) and the adjusted $r^2$ (0.95) was less than 0.2, which is reasonable. Adequate precision is a signal/noise ratio. It compares the range of the predicted values at the design points to average prediction error. Ratios greater than 4 indicate adequate model discrimination. The adequate precision obtained was 25.55, implying an adequate signal.

The F-values of the terms allow determining which component has greater effect on the response. The F-values of the model terms indicated that the moisture content of the samples was mainly affected by the chitosan concentration, followed by the

interaction between chitosan-PVOH. Equation 7 predicts the moisture content of the bacterial cellulose films as a function of chitosan and PVOH concentrations.

$$Moisture\ content\ (\%) = 1.72 + 10.57 \cdot Chitosan\ (\%) + 1.58 \cdot PVOH(\%) - 2.22 \cdot Chitosan(\%) \cdot PVOH(\%) \quad \text{(Eq. 7)}$$

According to the response surface (Figure 3a), the presence of chitosan or PVOH in bacterial cellulose films increased the moisture content. Mainly the chitosan is responsible for the increase of moisture content. This increase was due to the hydrophilic nature of the chitosan and PVOH. The chitosan effect was more significant due to its large amount of hydrophilic amino and hydroxyl groups. The moisture adsorption behaviour of chitosan-PVOH blends in different humidity environments were investigated in previous studies (Liu et al., 2018). Results in this study demonstrated a higher moisture content of the composites when increasing the chitosan concentration.

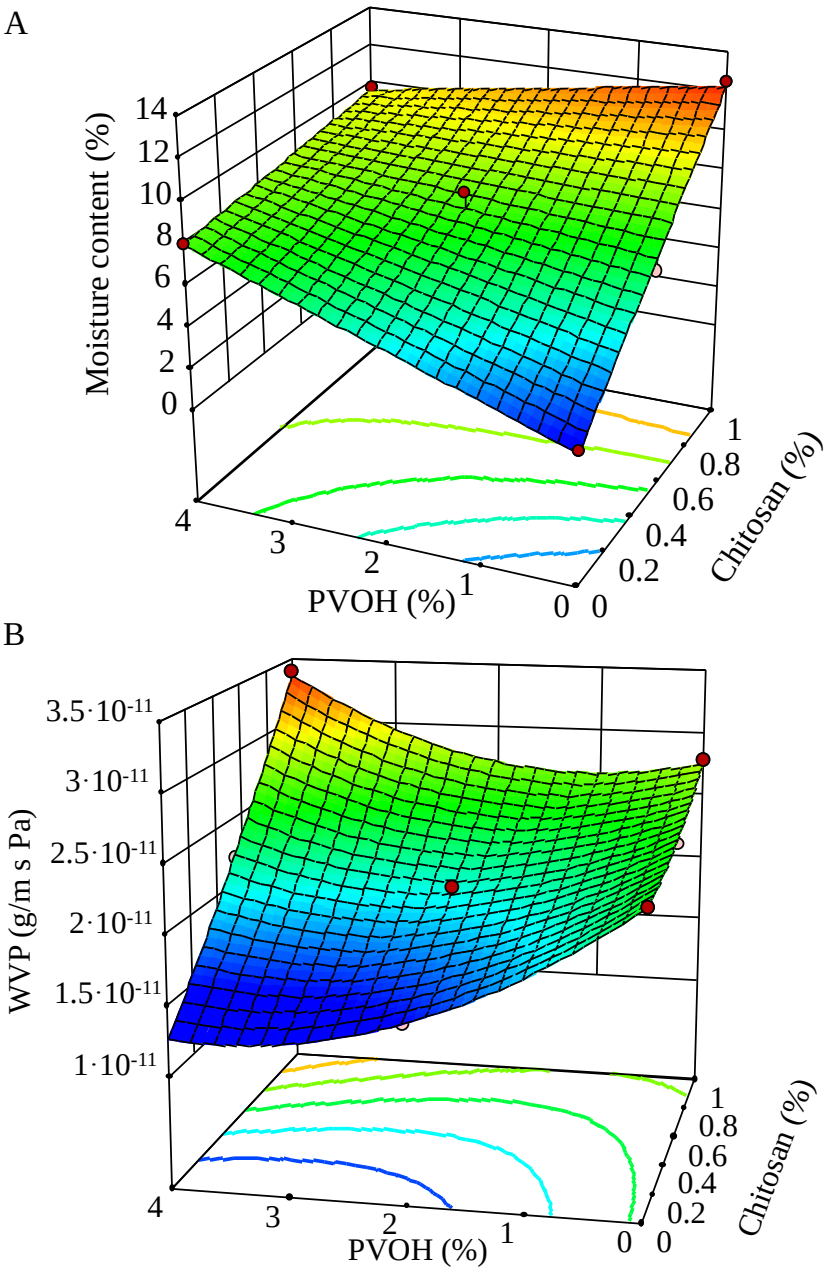


377

378

379 Fig. 3. Prediction of the model for the effect on A) moisture content in equilibrium and

380 B) water vapour permeability (WVP) of chitosan and poly(vinyl alcohol) on bacterial

381 cellulose films.

### *3.3. Water vapour permeability (WVP)*

The WVP values ranged from $1.47 \cdot 10^{-11}$ to $3.40 \cdot 10^{-11}$ g/m·s·Pa. Data were well fitted to a quadratic model. Experiment 3 was ignored because it was identified as an outlier by the Cook's distance test. The F-value of the model was 143.37 with a p-value of 0.0069, indicating that the mathematical model was significant. The value of $r^2$ was 0.99. The predicted $r^2$ (0.95) was in reasonable agreement with the adjusted $r^2$ (0.99). The adequate precision was higher than 4 (39.39), implying an adequate signal. The F-values indicate that the chitosan had the most important effect on the WVP response, followed by the interaction chitosan-PVOH.

Equation 8 predicts the response on WVP as a function of chitosan and PVOH.

$$WVP\ (g/m \cdot s \cdot Pa) = 2.38 \cdot 10^{-11} + 4.71 \cdot 10^{-13} \cdot Chitosan\ (\%) - 6.23 \cdot 10^{-12} \cdot PVOH(\%) + 4.30 \cdot 10^{-12} \cdot Chitosan(\%) \cdot PVOH(\%) + 3.45 \cdot 10^{-12} \cdot Chitosan(\%)^2 + 8.65 \cdot 10^{-13} \cdot PVOH(\%)^2 \quad \text{(Eq. 8)}$$

As shown in the response surface (Figure 3b), the WVP pattern depended on the components blended with the BC. BC-chitosan blends increased the WVP when the chitosan content increased. The hydrophilic property of the chitosan could explain the increase of WVP. Conversely, BC-PVOH films had lower permeability than pure cellulose films. Pure BC films showed a WVP of $2.38 \cdot 10^{-11}$ (g/m·s·Pa) and pure PVOH films reported a WVP of $1.70 \cdot 10^{-11}$ g/m·s·Pa at 30 ºC (Jipa et al., 2012). Pure BC films have an open porous structure, which facilitate the diffusion of the water molecules through cellulose fibers. Some voids between the cellulose fibers could have been filled by the PVOH decreasing the porosity and hindering the diffusion of the water

405 molecules. PVOH is a hydrophilic polymer, but its interaction capacity with water is
406 lower than that of chitosan (Liu et al., 2018). For this reason, bacterial cellulose-PVOH
407 films showed lower WVP values than that of bacterial cellulose-chitosan films.
408 However, this behaviour changed in presence chitosan-PVOH, producing a higher
409 increase of the permeability when the concentration of both polymers increased. This
410 effect has been reported in previous studies as chitosan-PVOH films manifested higher
411 WVP values than pure chitosan or PVOH films. The authors justified this effect as a
412 result of the formation of a more open matrix. The hydration layers of the chitosan
413 resulted in a lower density of the polymeric matrix. This structure facilitated the transfer
414 of water molecules through the network (Bonilla, Fortunati, Atarés, Chiralt, & Kenny,
415 2014). Regenerated cellulose-chitosan-PVOH films showed the same effect on WVP
416 (Cazón et al., 2018b).
417
418 *3.4. Mechanical properties*
419 The TS values ranged from 20.76 to 41.65 MPa. Data fitted well to a quadratic
420 equation. The F-value of the model was 30.63, indicating that the model was significant.
421 All terms in the quadratic model were significant ($p < 0.05$). The value of $r^2$ was 0.98
422 and the predicted $r^2$ was in reasonable agreement with the adjusted $r^2$. The adequate
423 precision obtained was 16.94, implying an adequate signal. The F-values of the model
424 terms indicated that TS was highly affected by the chitosan. Equation 9 forecasts the
425 values of TS as a function of chitosan and PVOH concentrations.
426

$$TS(MPa) = 20.99 + 33.90 \cdot Chitosan\ (\%) + 6.29 \cdot PVOH(\%) - 2.30 \cdot Chitosan(\%) \cdot PVOH(\%) - 16.33 \cdot Chitosan(\%)^2 - 1.09 \cdot PVOH(\%)^2 \quad \text{(Eq. 9)}$$

Pure regenerated cellulose film reported a TS value of 38.30 MPa from a dissolution of 4% of cellulose microcrystalline (Cazón et al., 2018b). Pure BC films showed a TS values of 20.76 MPa. BC films showed lower TS values than regenerated cellulose films, despite BC has higher crystallinity, because in its structure there are not remains of amorphous structures. There are two reasons responsible of this TS difference. One reason is the variation of the thickness. Pure regenerated cellulose studied was three folds thicker than pure BC films. Lower thickness could imply lower interaction among the cellulose fibers. It was observed that the TS values of the regenerated cellulose films depended on the cellulose concentration (Cazón et al., 2018b). In addition, bacterial cellulose had a less packed structure than regenerated cellulose, as shown the SEM images. These differences in the microstructure could affect the resistance to rupture, but also could promote the interaction with other polymers in the blend. Probably, longer fermentation time of the acetic bacteria to obtain thicker films, could help to increase the hydrogen bond interactions and increase the TS values. In literature, TS values have been reported between 5 and 96 MPa for pure BC films (Cai & Kim, 2010; Phisalaphong & Jatupaiboon, 2008; Saibuatong & Phisalaphong, 2010b; Szymańska-Chargot et al., 2017). The wide range of TS values could be explained because the properties of cellulose depend on the specific assembling and supramolecular order controlled by the culture medium, fermentation

conditions and treatment of cellulose. The measuring conditions or the moisture content of the samples also affect the obtained values (Hu et al., 2014).

On the other hand, analysing the interaction with other polymers, the addition of chitosan and/or PVOH increase in general the TS values of the films. The effect on TS of chitosan and PVOH is shown in the Figure 4a. TS values reported for pure chitosan films elaborated from an aqueous solution of acetic acid and similar storage conditions ranged from 50 to 70 MPa (Leceta, Guerrero, & De La Caba, 2013; Li, Zivanovic, Davidson, & Kit, 2010; Liu et al., 2018). Regarding pure PVOH films, the TS values reported ranged from 40 to 50 MPa (Hu & Wang, 2016; Liu et al., 2018; Lu, Wang, & Drzal, 2008).

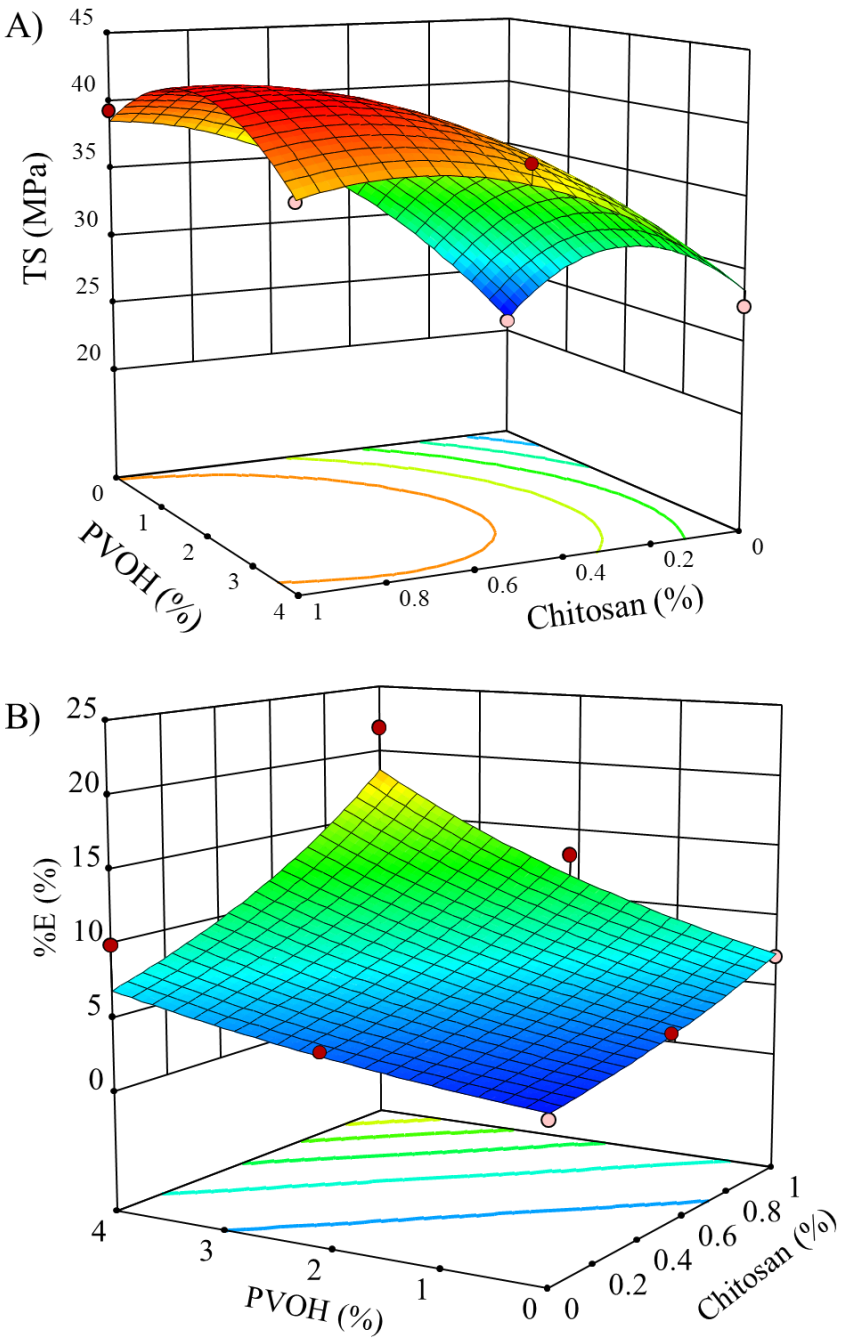


461

462 Fig. 4. Prediction of the model for the effect on A) the tensile strength (TS) and B)

463 percentage of elongation at break (%E) of chitosan and poly(vinyl alcohol) on bacterial

464 cellulose films.

465

Both polymers reported higher TS values than pure BC. Thus, films were reinforced after combining BC with polymers with higher TS values. New physical interactions among the components took place, due to the possibility interaction between -OH and -$NH_2$ groups in these polymers. These new physical interactions were able to improve the mechanical properties of the blend films (Bahrami, Kordestani, Mirzadeh, & Mansoori, 2003; Bonilla et al., 2014). Besides, as observed in the SEM images, the presence of PVOH and chitosan increased the density of the structure, obtaining a more compact structure, which explain the increase of TS. However, at the highest chitosan and PVOH concentrations, TS decreased slightly, but maintained higher values than those of pure BC. This change was due to the increase of the moisture content of the samples due to the hydrophilic nature of chitosan and PVOH. The water had a plasticizing effect on the polymers, promoting the mobility of the polymeric chains (Liu et al., 2018). Higher incubation times (14 days) and freeze drying (−40 °C for 3 days), modified the structure of BC-chitosan films, modified the mechanical properties and allowed obtaining TS values of 450 MPa (Kim et al., 2011).

The %E values ranged from 2.28 to 21.82%. Data fitted well to a linear model. The Box-Cox plot recommended transforming the data to logarithmic base 10 of %E to get a better fit of the equation. The F-value of the model was 9.80, indicating that the model is significant. There is only a 1.29% chance that a F-value could be due to noise. All model terms were significant ($p < 0.05$) and the value of $r^2$ was 0.77. In this case, the predicted $r^2$ of 0.48 was slightly away from the adjusted $r^2$ of 0.69. However, the adequate precision obtained was 8.85, indicating an adequate signal to noise ratio. The F-values of the model terms indicated that chitosan produced a slightly higher effect on

the %E. Equation 10 predicts the %E response as a function of the chitosan and PVOH concentrations.

$$Log_{10}(\%E) = 0.41 + 0.43 \cdot Chitosan\ (\%) + 0.10 \cdot PVOH(\%) \qquad \text{(Eq. 10)}$$

Reported %E values for pure BC ranges from 0.6 to 5% (Cai & Kim, 2010). According to the response surface (Figure 4b), the presence of chitosan or PVOH in BC films increased the %E values. This behaviour was more significant in formulations containing chitosan and PVOH. The %E of pure BC films was 2.28%, higher than that of regenerated cellulose (1.55%) (Cazón et al., 2018b). The higher %E of BC allowed an easier manipulation than that of regenerated cellulose. Developed films in this study significantly increased the elasticity up to a maximum value of 21.82% when chitosan and PVOH were added. This increase in elasticity facilitated the manipulation of the films. Besides, adding chitosan and PVOH increased the moisture content which had an plasticizing effect on the film (Liu et al., 2018; Suyatma, Tighzert, Copinet, & Coma, 2005). Probably the interaction of cellulose fibres with PVOH and water molecules reduced the frictional forces between polymeric chains, facilitating their mobility. In addition, new interactions cellulose-chitosan-PVOH-water through hydrogen bonds could modify the elasticity of the polymer (Liu et al., 2018; Suyatma et al., 2005). Regenerated cellulose-chitosan-PVOH films reached a maximum elasticity of 12.82% (Cazón et al., 2018b), lower than the bacterial cellulose-chitosan-PVOH films. This result suggests that the more open three-dimensional structure of the BC promoted the interaction among the polymers in the composite film. On the other hand the percentage

512 of elongation at break of the composite films was superior to the individual component,
513 probably promoted by the physical interaction of chitosan-PVOH in the blends (Liu et
514 al., 2018).

515 The Young's modulus values obtained were in the range from 1043.88 to
516 2247.82 MPa. Data fitted well to a quadratic equation. Trial 7 was disregarded because
517 it was identified as an outlier by the Cook's distance test. The F-value of the model was
518 302.83 with a p-value = 0.0033. These statistical parameters indicated that the
519 mathematical model was significant. The value of $r^2$ was 0.99 and the adjusted $r^2$
520 (0.99) was in reasonable agreement with the predicted $r^2$ (0.98). The adequate precision
521 value was higher than 4 (48.82), implying an adequate signal to noise ratio. F-values
522 indicated that the quadratic effect of chitosan and PVOH content had the most important
523 effect on the response of %E, followed by the linear effect of the PVOH. Equation 11
524 predicts the response on Young's Modulus as a function of the components of chitosan
525 and PVOH.

526

527 $$Young`s\ Modulus\ (MPa) = 1034.58 + 2301.07 \cdot Chitosan\ (\%) + 579.66 \cdot$$
528 $$PVOH(\%) + 189.12 \cdot Chitosan(\%) \cdot PVOH(\%) - 2929.43 \cdot Chitosan(\%)^2 -$$
529 $$144.35 \cdot PVOH(\%)^2 \qquad \text{(Eq.11)}$$

530

531 According to the response surface (Figure 5), YM values increased when the
532 concentration of chitosan and PVOH increased up to intermediate values. This
533 behaviour could be explained due to the intermolecular hydrogen bonds formed among
534 the components in the film. Similar results were observed in regenerated cellulose-

chitosan-PVOH (Cazón et al., 2018b). However, if the concentration of chitosan and PVOH continued increasing, YM values decreased, especially with the increasing of chitosan. Also, the increase of moisture content in the films significantly decreased the YM values. The effect of water on YM has been reported in chitosan-PVOH film. In general, YM values of pure chitosan film range from 1500 to 3000 MPa, depending on the chitosan concentration, molecular weight, solvent, deacetylation degree and storage conditions (Fernandes et al., 2010; Liu et al., 2018). YM values for PVOH films range from 1000-1500 MPa (Paralikar, Simonsen, & Lombardi, 2008; Roohani et al., 2008). However, these values dropped to 60 MPa and 5 MPa, respectively when conditioning the films at high relative humidity (75% RH), demonstrating the effect of water molecules on the YM (Liu et al., 2018).

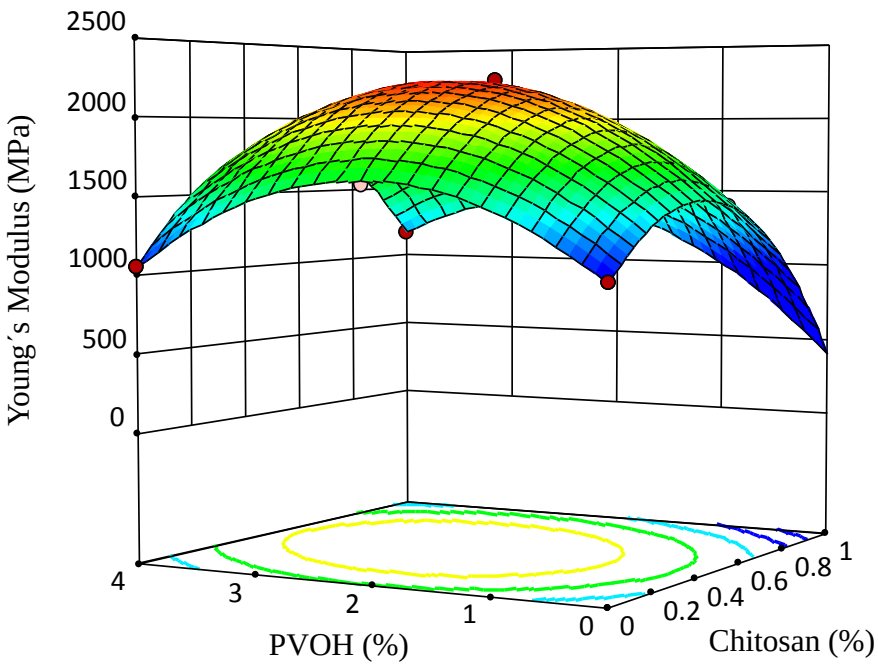

549 Fig. 5. Prediction of the model for the effect on the Young´s Modulus of chitosan and
550 poly(vinyl alcohol) on bacterial cellulose films.
551
552 *3.5. Light barrier properties, transparency and opacity*
553 One of the main objectives of active packaging is maintaining the quality of
554 food to increase the shelf life. Hence, to develop biofilms with good optical barrier in
555 the region of UV-radiation is a feasible strategy. UV-light is the main responsible for
556 the appearance of the singlet oxygen, the most common cause of lipid oxidation. This
557 oxidative reaction alters the odour, taste and colour of food, diminishing its organoleptic
558 qualities, that affect the acceptability of food to consumers (Goudarzi, Shahabi-
559 Ghahfarrokhi, & Babaei-Ghazvini, 2017; Vilela et al., 2017). On the other hand,
560 biodegradable films with UV-light barriers properties should have an adequate
561 transparency. Biopolymers with good values of transparency applied directly on food
562 provide a good visual appearance, increasing their consumer acceptancy (Cazón et al.,
563 2018a).
564 The lipids are more susceptible to oxidative reactions in the region from 200 to
565 280 nm wavelength. Figure 6a shows the transmittance of the experiments 1, 3 and 7 in
566 the 200-280 nm UV range. The select samples allow to analyse the optical properties of
567 pure bacterial cellulose, and the effect of the PVOH and chitosan on the composite
568 films. In this region, pure bacterial cellulose showed transmittance values of 0% up to a
569 wavelength of 230 nm, then increasing up to 2%. Pure bacterial cellulose films showed
570 lower transmittance values than pure regenerated cellulose which ranged from 0.4 to
571 5.3% (Cazón et al., 2018a). This difference is probably due to the purity of the BC and

572 the structural differences between the films. The addition of PVOH increased the
573 transmittance at 210 nm up to 11.65%. BC-chitosan spectra showed that the
574 transmittance values remained low, without significant differences when compared to
575 pure bacterial cellulose. In previous studies, chitosan showed lower transmittance
576 values in the UV region between 200 and 280 nm (Kalaycıoğlu, Torlak, Akın-Evingür,
577 Özen, & Erim, 2017; Kanatt et al., 2012). That is the reason because BC-chitosan films
578 kept the low values.

579 In the UV-VIS region (280– 800 nm) (Figure 6b), pure BC films kept low values
580 of transmittance, with a maximum transmittance of 11%. Adding PVOH to BC resulted
581 in the greatest effect on transmittance, increasing the value up 46.6%. However, in
582 chitosan-BC samples, the transmittance increased constantly with the wavelength, up to
583 32%. This increase of the transmittance affected the visual properties modifying the
584 transparency and opacity of the films.

585

586

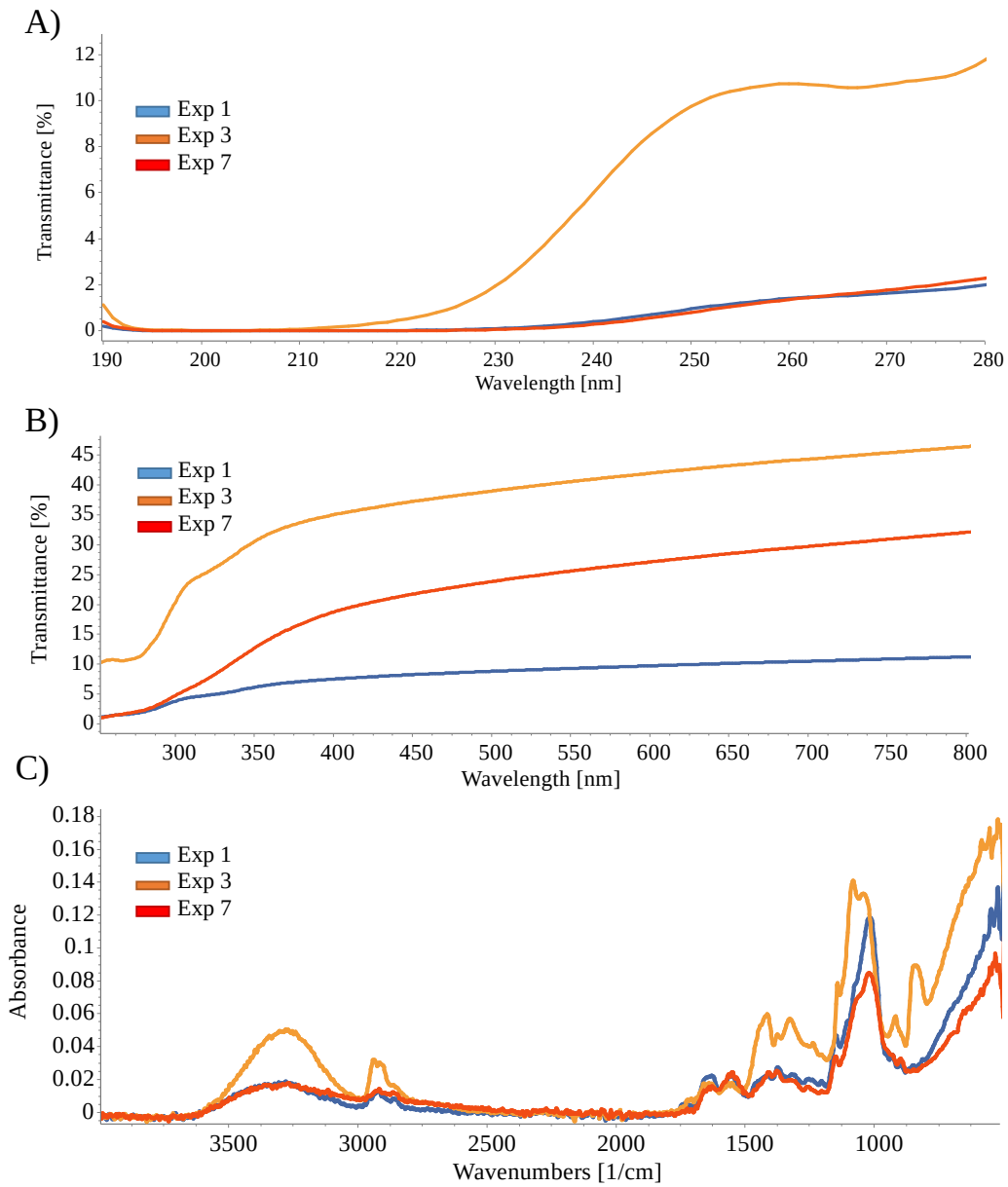


587

588

589 Fig. 6. Spectra profile A) and B) of UV-VIS and C) FT-IR of films from experiments 1,

590 3 and 7: Exp 1) Pure bacterial cellulose sample; Exp 3) Bacterial cellulose-poly(vinyl

591 alcohol) 4% (w/w); Exp 7) Bacterial cellulose-chitosan 1% (w/w).

592

Pure cellulose films had a smoked colour, but the formulations with PVOH resulted in films with a translucent and shiny appearance. However, the transparency values obtained for samples 1, 3 and 7 were 47.6, 24.5 and 48.0, respectively. According to these results, pure BC film had the best transparency value, followed by the chitosan film and then PVOH film. These values were strongly affected by the thickness. Films with PVOH were three times thicker than pure BC samples. BC-chitosan films were twice as thick as pure BC. For this reason, it is necessary to complete this information with the opacity. The opacity values calculated were 50.9, 6.2 and 20.9 for pure BC, BC-PVOH and BC-chitosan films, respectively. The transparency and opacity values indicate that the PVOH, followed by the chitosan, improved the optical properties of the films in the visible region, thus improving their appearance as shown in Figure 7. In this region, the transmittance values were slightly lower than the values obtained for regenerated cellulose-chitosan-PVOH films previously studied (Cazón et al., 2018a).

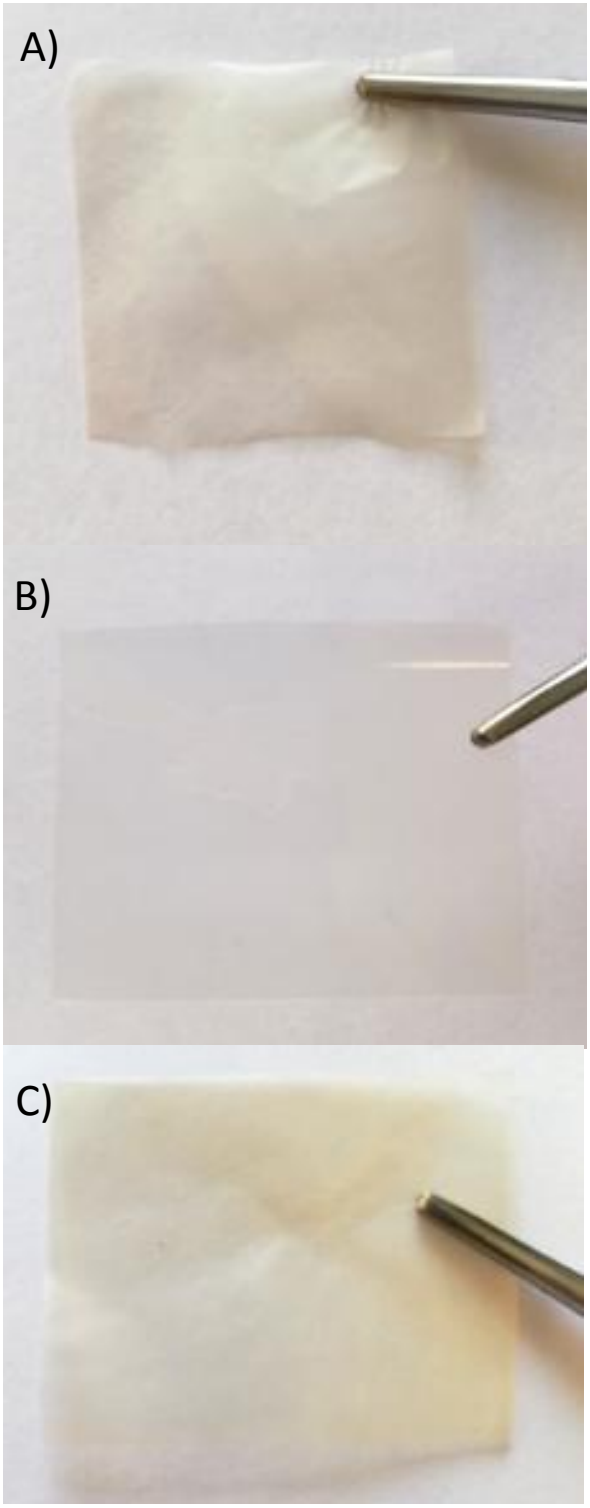


608

609 Fig. 7. Visual appearance of the A) pure bacterial cellulose sample, B) bacterial

610 cellulose-poly(vinyl alcohol) 4% (w/w) and C) bacterial cellulose-chitosan 1% (w/w).

### *3.6. Fourier transform infrared spectroscopy (FT-IR)*

The interactions between BC-PVOH-chitosan at structural level were evaluated by FT-IR measurements. Figure 6c shows the FT-IR spectra of the experiment 1, 3 and 7. The spectra show the characteristic absorption bands of BC, PVOH and chitosan. A broad band in the 3000–3600 $cm^{-1}$ region is attributed to the intermolecular hydrogen bonding and -OH stretching vibrations in BC and PVOH. The addition of PVOH resulted in a slight displacement of this peak at a higher wavenumber, probably due to the increase of -OH groups and the formation of hydrogen bonding. The -NH stretching vibration of chitosan is also located in this region. This increase of the absorbance could also be associated to the interaction with -OH group (Cazón et al., 2018a; Pavaloiu, Stoica-Guzun, Stroescu, Jinga, & Dobre, 2014). A weak signal at 2920 $cm^{-1}$ appeared in the three samples, due to the -CH stretching.

The absorbance peaks observed around 1550 $cm^{-1}$ were assigned to $-NH_2$ deformation vibration of chitosan (Zhao, Teixeira, Gänzle, & Saldaña, 2018). However, FT-IR spectra of pure BC and BC-PVOH films showed a peak of absorbance at 1550 $cm^{-1}$, with lower intensity. Probably, due to the presence of residues from the culture medium that could not be completely removed during the washing process, since films elaborated with regenerated cellulose did not show absorbance at this wavelength (Cazón et al., 2018a). The absorption bands with a maximum at 1055 $cm^{-1}$ and 1020 $cm^{-1}$ are assigned to the C-O-C pyranose ring stretching vibrations and C-H ring deformation, respectively. In this region, the BC-PVOH bands are shifted in comparison

633 to the pure BC spectra, indicating polymeric association through hydrogen bonding
634 (Pereira, de Arruda, & Stefani, 2015).
635
636 *3.7. Thermal properties of films TGA-DSC*
637 Thermogravimetry and differential scanning calorimetry of the samples from the
638 experiments 1, 3 and 7 were carried out simultaneously. These measurements allowed
639 assessing the stability of pure BC and the effect of adding PVOH and chitosan on the
640 thermal stability of the films. Figure 8 shows the thermograms obtained for each
641 sample. The first endothermic peak (60 - 110)°C corresponded to the volatilization of
642 water from the films samples (Martins et al., 2009). In agreement with the data obtained
643 in the measurement of moisture content in equilibrium, this first peak resulted in a
644 weight loss of 3.4, 3.9 and 5.3%, for the pure BC, BC-PVOH and BC-chitosan films,
645 respectively.
646
647

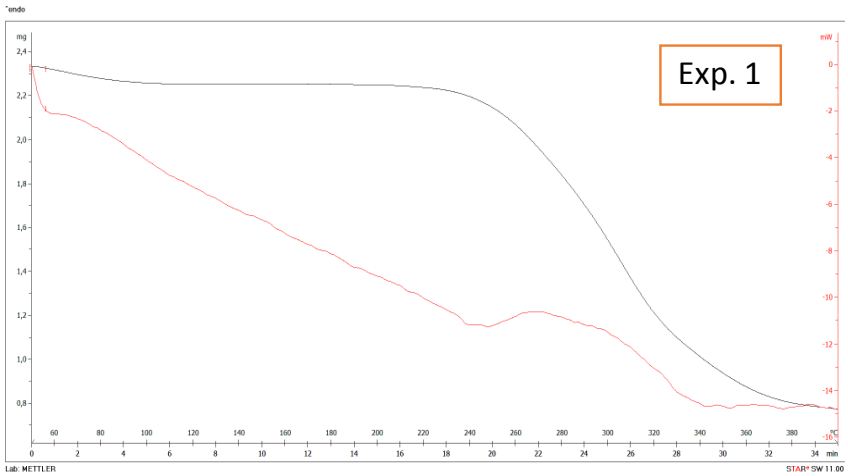
Exp. 1
Lab: METTLER
STAR° SW 11.00

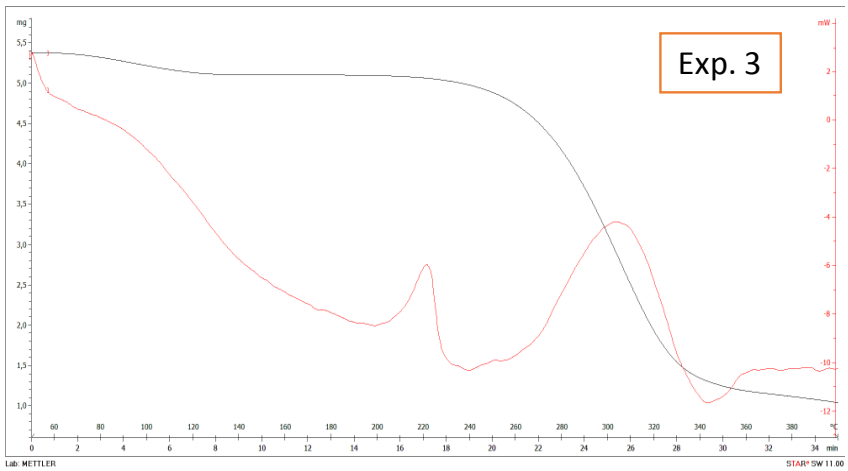
Exp. 3
Lab: METTLER
STAR° SW 11.00

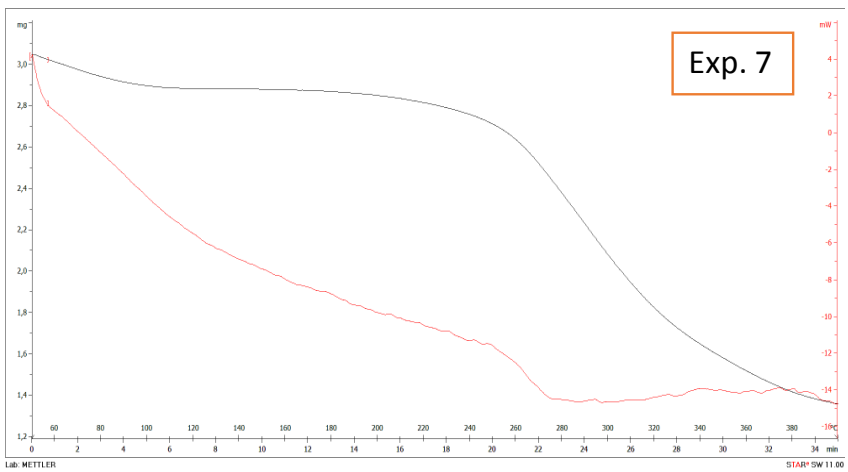
Exp. 7
Lab: METTLER
STAR° SW 11.00

648

649

Fig. 8. Thermogravimetry and differential scanning calorimetry of experiments 1, 3 and 7: 1) Pure bacterial cellulose sample; 3) Bacterial cellulose-poly(vinyl alcohol) 4% (w/w); 7) Bacterial cellulose-chitosan 1% (w/w).

In Figure 8, the endothermic peak at 250°C corresponded to the onset temperature of thermal degradation of cellulose, in accordance with the data observed in previous works (Mohammadkazemi et al., 2015). At 400 °C the decomposition of the BC corresponded to the 66.7% of the weight loss. The thermogram of the BC-PVOH samples showed two endothermic peaks in the second region. The first endothermic peak, at about 220 °C, corresponds to the thermal degradation of PVA (Bonilla et al., 2014). In the 200-240 ºC range, the percentage of the weight loss was 5.2-7.2% of the total initial weight. The loss of weight in this interval was not significant, which indicated that part of PVOH, degraded at higher temperatures probably due to the interaction with cellulose. The second endothermic peak, at 260-340 ºC, corresponded to the 11.1-74.4% weight loss of the initial weight. Data suggest that the BC-PVOH interaction increased the thermal stability of the films, increasing the degradation temperature of the PVOH and the BC. On the other hand, in presence of chitosan, the degradation onset temperature of the sample was found in the 260-270 ºC region. The presence of chitosan increased the degradation temperature of the sample compared to that of pure BC. At the 260-340 ºC region, the weight loss was 12.7-45.0%, reaching a weight loss of 55.1% up to a temperature of 400 ºC, indicating that the interaction BC-chitosan increased the thermal stability the sample. Regenerated cellulose-PVOH and

672 regenerated cellulose-chitosan also showed this increase in thermal stability due to the
673 interaction between the polymers (Cazón et al., 2018a).
674
675 **4. Conclusions**
676 Results showed that it is feasible to obtain BC-based films with potential
677 applications as active biopolymer for food packaging. Combining BC with PVOH and
678 chitosan allowed improving or modifying the mechanical, vapour permeability, thermal
679 and optical properties of the films. The equilibrium moisture content had an important
680 effect on the mechanical properties of the films. TS and %E values of the samples
681 increased with the presence of PVOH and chitosan. WVP decreased slightly when
682 PVOH was added into the formulation. Chitosan increased the permeability of the films.
683 PVOH and chitosan decreased the porosity of the BC films and increased the films
684 density. The UV-VIS spectra showed the optimal optical barrier properties of BC-based
685 films against UV-radiation. Adding PVOH increased the transmittance values in the
686 UV-VIS region and improved the transparency and visual appearance of the films. FT-
687 IR and TGA-DSC indicated the interaction among the polymers. These properties could
688 be useful in food industry as an alternative to synthetic film preventing the lipid
689 oxidations in foods.
690
691 **Acknowledgements**
692 A grant from CONACYT (México) (#435948) to author Patricia Cazón is
693 gratefully acknowledged. The financial support for this project was provided by
694 Consellería de Cultura, Educación e Ordenación Universitaria, Xunta de Galicia (ES)

(Project # ED431B 2016/009). Authors would like to thank the use of RIAIDT-USC analytical facilities.

## References

Antoniou, J., Liu, F., Majeed, H., & Zhong, F. (2015). Characterization of tara gum edible films incorporated with bulk chitosan and chitosan nanoparticles: A comparative study. *Food Hydrocolloids*, *44*, 309–319. https://doi.org/http://dx.doi.org/10.1016/j.foodhyd.2014.09.023

Bahrami, S. B., Kordestani, S. S., Mirzadeh, H., & Mansoori, P. (2003). Poly (vinyl alcohol) - Chitosan Blends: Preparation, Mechanical and Physical Properties. *Iranian Polymer Journal*, *12*(2), 139–146.

Bonilla, J., Fortunati, E., Atarés, L., Chiralt, A., & Kenny, J. M. (2014). Physical, structural and antimicrobial properties of poly vinyl alcohol-chitosan biodegradable films. *Food Hydrocolloids*, *35*, 463–470. https://doi.org/10.1016/j.foodhyd.2013.07.002

Broek Van Den, L. A. M., Knoop, R. J. I., Kappen, F. H. J., & Boeriu, C. G. (2015). Chitosan films and blends for packaging material. *Carbohydrate Polymers*, *116*, 237–242. https://doi.org/10.1016/j.carbpol.2014.07.039

Brown, E. E., & Laborie, M.-P. G. (2007). Bioengineering Bacterial Cellulose/Poly(ethylene oxide) Nanocomposites. *Biomacromolecules*, *8*(10), 3074–3081. https://doi.org/10.1021/bm700448x

Cai, Z., & Kim, J. (2010). Bacterial cellulose/poly(ethylene glycol) composite: Characterization and first evaluation of biocompatibility. *Cellulose*, *17*(1), 83–91.

https://doi.org/10.1007/s10570-009-9362-5

Carvalho, R. A., Maria, T. M. C., Moraes, I. C. F., Bergo, P. V. A., Kamimura, E. S., Habitante, A. M. Q. B., & Sobral, P. J. A. (2009). Study of some physical properties of biodegradable films based on blends of gelatin and poly(vinyl alcohol) using a response-surface methodology. *Materials Science and Engineering: C*, *29*(2), 485–491. https://doi.org/10.1016/J.MSEC.2008.08.030

Cazón, P., Vázquez, M., & Velazquez, G. (2018a). Composite films of regenerate cellulose with chitosan and polyvinyl alcohol: Evaluation of water adsorption, mechanical and optical properties. *International Journal of Biological Macromolecules*, *117*, 235–246. https://doi.org/10.1016/j.ijbiomac.2018.05.148

Cazón, P., Vázquez, M., & Velazquez, G. (2018b). Novel composite films based on cellulose reinforced with chitosan and polyvinyl alcohol: Effect on mechanical properties and water vapour permeability. *Polymer Testing*, *69*(June), 536–544. https://doi.org/10.1016/j.polymertesting.2018.06.016

Cazón, P., Velazquez, G., Ramírez, J. A., & Vázquez, M. (2017). Polysaccharide-based films and coatings for food packaging: A review. *Food Hydrocolloids*, *68*, 136–148. https://doi.org/10.1016/j.foodhyd.2016.09.009

Cook, R. D. (1977). Detection of Influential Observations in Linear Regression. *Technometrics*, *19*(1), 15–18. https://doi.org/10.2307/1268249

Fernandes, S. C. M., Freire, C. S. R., Silvestre, A. J. D., Pascoal Neto, C., Gandini, A., Berglund, L. A., & Salmén, L. (2010). Transparent chitosan films reinforced with a high content of nanofibrillated cellulose. *Carbohydrate Polymers*, *81*(2), 394–401. https://doi.org/10.1016/j.carbpol.2010.02.037

741 Gea, S., Bilotti, E., Reynolds, C. T., Soykeabkeaw, N., & Peijs, T. (2010). Bacterial
742 cellulose–poly(vinyl alcohol) nanocomposites prepared by an in-situ process.
743 *Materials Letters*, *64*(8), 901–904.
744 https://doi.org/10.1016/J.MATLET.2010.01.042
745 Gennadios, A., Weller, C. L., & Gooding, C. H. (1994). Measurement Errors in Water-
746 Vapor Permeability of Highly Permeable, Hydrophilic Edible Films. *Journal of*
747 *Food Engineering*, *21*(4), 395–409. https://doi.org/Doi 10.1016/0260-
748 8774(94)90062-0
749 George, J., & Siddaramaiah. (2012). High performance edible nanocomposite films
750 containing bacterial cellulose nanocrystals. *Carbohydrate Polymers*, *87*(3), 2031–
751 2037. https://doi.org/10.1016/j.carbpol.2011.10.019
752 Goudarzi, V., Shahabi-Ghahfarrokhi, I., & Babaei-Ghazvini, A. (2017). Preparation of
753 ecofriendly UV-protective food packaging material by starch/TiO2bio-
754 nanocomposite: Characterization. *International Journal of Biological*
755 *Macromolecules*, *95*, 306–313. https://doi.org/10.1016/j.ijbiomac.2016.11.065
756 Han, J. H., & Floros, J. D. (1997). Casting Antimicrobial Packaging Films and
757 Measuring Their Physical Properties and Antimicrobial Activity. *Journal of Plastic*
758 *Film & Sheeting*, *13*(4), 287–298. https://doi.org/10.1177/875608799701300405
759 Helander, I. M., Nurmiaho-Lassila, E. L., Ahvenainen, R., Rhoades, J., & Roller, S.
760 (2001). Chitosan disrupts the barrier properties of the outer membrane of Gram-
761 negative bacteria. *International Journal of Food Microbiology*, *71*(2–3), 235–244.
762 https://doi.org/10.1016/S0168-1605(01)00609-2
763 Hu, D., & Wang, L. (2016). Fabrication of antibacterial blend film from poly (vinyl

764 alcohol) and quaternized chitosan for packaging. *Materials Research Bulletin*, *78*,
765 46–52. https://doi.org/10.1016/J.MATERRESBULL.2016.02.025
766 Hu, W., Chen, S., Yang, J., Li, Z., & Wang, H. (2014). Functionalized bacterial
767 cellulose derivatives and nanocomposites. *Carbohydrate Polymers*, *101*, 1043–
768 1060. https://doi.org/10.1016/j.carbpol.2013.09.102
769 Jipa, I. M., Stroescu, M., Stoica-Guzun, A., Dobre, T., Jinga, S., & Zaharescu, T.
770 (2012). Effect of gamma irradiation on biopolymer composite films of poly(vinyl
771 alcohol) and bacterial cellulose. *Nuclear Instruments and Methods in Physics*
772 *Research, Section B: Beam Interactions with Materials and Atoms*, *278*, 82–87.
773 https://doi.org/10.1016/j.nimb.2012.02.024
774 Jozala, A. F., de Lencastre-Novaes, L. C., Lopes, A. M., de Carvalho Santos-Ebinuma,
775 V., Mazzola, P. G., Pessoa-Jr, A., … Chaud, M. V. (2016). Bacterial nanocellulose
776 production and application: a 10-year overview. Springer Verlag.
777 https://doi.org/10.1007/s00253-015-7243-4
778 Kalaycıoğlu, Z., Torlak, E., Akın-Evingür, G., Özen, İ., & Erim, F. B. (2017).
779 Antimicrobial and physical properties of chitosan films incorporated with turmeric
780 extract. *International Journal of Biological Macromolecules*, *101*, 882–888.
781 https://doi.org/10.1016/J.IJBIOMAC.2017.03.174
782 Kanatt, S. R., Rao, M. S., Chawla, S. P., & Sharma, A. (2012). Active chitosan–
783 polyvinyl alcohol films with natural extracts. *Food Hydrocolloids*, *29*(2), 290–297.
784 https://doi.org/10.1016/J.FOODHYD.2012.03.005
785 Kim, J., Cai, Z., Lee, H. S., Choi, G. S., Lee, D. H., & Jo, C. (2011). Preparation and
786 characterization of a Bacterial cellulose/Chitosan composite for potential

biomedical application. *Journal of Polymer Research*, *18*(4), 739–744. https://doi.org/10.1007/s10965-010-9470-9

Leceta, I., Guerrero, P., & De La Caba, K. (2013). Functional properties of chitosan-based films. *Carbohydrate Polymers*, *93*(1), 339–346. https://doi.org/10.1016/j.carbpol.2012.04.031

Li, J., Zivanovic, S., Davidson, P. M., & Kit, K. (2010). Characterization and comparison of chitosan/PVP and chitosan/PEO blend films. *Carbohydrate Polymers*, *79*(3), 786–791. https://doi.org/10.1016/J.CARBPOL.2009.09.028

Liu, L., Liang, H., Zhang, J., Zhang, P., Xu, Q., Lu, Q., & Zhang, C. (2018). Poly(vinyl alcohol)/Chitosan composites: Physically transient materials for sustainable and transient bioelectronics. *Journal of Cleaner Production*, *195*, 786–795. https://doi.org/10.1016/j.jclepro.2018.05.216

Lu, J., Wang, T., & Drzal, L. T. (2008). Preparation and properties of microfibrillated cellulose polyvinyl alcohol composite materials. *Composites Part A: Applied Science and Manufacturing*, *39*(5), 738–746. https://doi.org/10.1016/j.compositesa.2008.02.003

Lucyszyn, N., Ono, L., Lubambo, A. F., Woehl, M. A., Sens, C. V., de Souza, C. F., & Sierakowski, M. R. (2016). Physicochemical and in vitro biocompatibility of films combining reconstituted bacterial cellulose with arabinogalactan and xyloglucan. *Carbohydrate Polymers*, *151*, 889–898. https://doi.org/10.1016/J.CARBPOL.2016.06.027

Martínez-Sanz, M., Lopez-Rubio, A., & Lagaron, J. M. (2013). High-barrier coated bacterial cellulose nanowhiskers films with reduced moisture sensitivity.

*Carbohydrate Polymers*, *98*(1), 1072–1082. https://doi.org/10.1016/J.CARBPOL.2013.07.020

Martins, I. M. G., Magina, S. P., Oliveira, L., Freire, C. S. R., Silvestre, A. J. D., Neto, C. P., & Gandini, A. (2009). New biocomposites based on thermoplastic starch and bacterial cellulose. *Composites Science and Technology*, *69*(13), 2163–2168. https://doi.org/10.1016/J.COMPSCITECH.2009.05.012

Mohammadkazemi, F., Azin, M., & Ashori, A. (2015). Production of bacterial cellulose using different carbon sources and culture media. *Carbohydrate Polymers*, *117*, 518–523. https://doi.org/10.1016/j.carbpol.2014.10.008

Moreira, M. del R., Roura, S. I., & Ponce, A. (2011). Effectiveness of chitosan edible coatings to improve microbiological and sensory quality of fresh cut broccoli. *LWT - Food Science and Technology*, *44*(10), 2335–2341. https://doi.org/10.1016/j.lwt.2011.04.009

No, H. K., Meyers, S. P., Prinyawiwatkul, W., & Xu, Z. (2007). Applications of chitosan for improvement of quality and shelf life of foods: A review. *Journal of Food Science*, *72*(5). https://doi.org/10.1111/j.1750-3841.2007.00383.x

Numata, Y., Sakata, T., Furukawa, H., & Tajima, K. (2015). Bacterial cellulose gels with high mechanical strength. *Materials Science and Engineering: C*, *47*, 57–62. https://doi.org/10.1016/j.msec.2014.11.026

Olarte, C., Sanz, S., Federico Echávarri, J., & Ayala, F. (2009). Effect of plastic permeability and exposure to light during storage on the quality of minimally processed broccoli and cauliflower. *LWT - Food Science and Technology*, *42*(1), 402–411. https://doi.org/10.1016/J.LWT.2008.07.001

833 Paralikar, S. A., Simonsen, J., & Lombardi, J. (2008). Poly(vinyl alcohol)/cellulose
834 nanocrystal barrier membranes. *Journal of Membrane Science*, *320*(1), 248–258.
835 https://doi.org/10.1016/j.memsci.2008.04.009
836 Pavaloiu, R.-D., Stoica-Guzun, A., Stroescu, M., Jinga, S. I., & Dobre, T. (2014).
837 Composite films of poly(vinyl alcohol)–chitosan–bacterial cellulose for drug
838 controlled release. *International Journal of Biological Macromolecules*, *68*, 117–
839 124. https://doi.org/10.1016/J.IJBIOMAC.2014.04.040
840 Pavaloiu, R. D., Dobre, T., & Hlevca, C. (2013). Use of bacterial cellulose-glycerol-
841 poly(vinyl alcohol) composites in drug release. *2013 E-Health and Bioengineering*
842 *Conference (EHB)*. https://doi.org/10.1109/EHB.2013.6707312
843 Pereira, V. A., de Arruda, I. N. Q., & Stefani, R. (2015). Active chitosan/PVA films
844 with anthocyanins from Brassica oleraceae (Red Cabbage) as Time–Temperature
845 Indicators for application in intelligent food packaging. *Food Hydrocolloids*, *43*,
846 180–188. https://doi.org/10.1016/J.FOODHYD.2014.05.014
847 Phisalaphong, M., & Jatupaiboon, N. (2008). Biosynthesis and characterization of
848 bacteria cellulose–chitosan film. *Carbohydrate Polymers*, *74*(3), 482–488.
849 https://doi.org/10.1016/J.CARBPOL.2008.04.004
850 Roohani, M., Habibi, Y., Belgacem, N. M., Ebrahim, G., Karimi, A. N., & Dufresne, A.
851 (2008). Cellulose whiskers reinforced polyvinyl alcohol copolymers
852 nanocomposites. *European Polymer Journal*, *44*(8), 2489–2498.
853 https://doi.org/10.1016/J.EURPOLYMJ.2008.05.024
854 Ruka, D. R., Simon, G. P., & Dean, K. M. (2012). Altering the growth conditions of
855 Gluconacetobacter xylinus to maximize the yield of bacterial cellulose.

*Carbohydrate Polymers*, *89*(2), 613–622. https://doi.org/10.1016/j.carbpol.2012.03.059

Saibuatong, O., & Phisalaphong, M. (2010a). Novo aloe vera–bacterial cellulose composite film from biosynthesis. *Carbohydrate Polymers*, *79*(2), 455–460. https://doi.org/10.1016/J.CARBPOL.2009.08.039

Saibuatong, O., & Phisalaphong, M. (2010b). Novo aloe vera–bacterial cellulose composite film from biosynthesis. *Carbohydrate Polymers*, *79*(2), 455–460. https://doi.org/10.1016/j.carbpol.2009.08.039

Sakia, R. M. (1992). The Box-Cox Transformation Technique: A Review. *The Statistician*, *41*(2), 169. https://doi.org/10.2307/2348250

Salari, M., Sowti Khiabani, M., Rezaei Mokarram, R., Ghanbarzadeh, B., & Samadi Kafil, H. (2018). Development and evaluation of chitosan based active nanocomposite films containing bacterial cellulose nanocrystals and silver nanoparticles. *Food Hydrocolloids*, *84*, 414–423. https://doi.org/10.1016/J.FOODHYD.2018.05.037

Shabanpour, B., Kazemi, M., Ojagh, S. M., & Pourashouri, P. (2018). Bacterial cellulose nanofibers as reinforce in edible fish myofibrillar protein nanocomposite films. *International Journal of Biological Macromolecules*, *117*, 742–751. https://doi.org/10.1016/J.IJBIOMAC.2018.05.038

Shah, N., Ul-Islam, M., Khattak, W. A., & Park, J. K. (2013). Overview of bacterial cellulose composites: A multipurpose advanced material. *Carbohydrate Polymers*, *98*(2), 1585–1598. https://doi.org/10.1016/j.carbpol.2013.08.018

Shao, W., Wang, S., Liu, H., Wu, J., Zhang, R., Min, H., & Huang, M. (2016).

879 Preparation of bacterial cellulose/graphene nanosheets composite films with
880 enhanced mechanical performances. *Carbohydrate Polymers*, *138*, 166–171.
881 https://doi.org/10.1016/J.CARBPOL.2015.11.033
882 Suyatma, N. E., Tighzert, L., Copinet, A., & Coma, V. (2005). Effects of hydrophilic
883 plasticizers on mechanical, thermal, and surface properties of chitosan films.
884 *Journal of Agricultural and Food Chemistry*, *53*(10), 3950–3957.
885 https://doi.org/10.1021/jf048790+
886 Szymańska-Chargot, M., Chylińska, M., Cybulska, J., Kozioł, A., Pieczywek, P. M., &
887 Zdunek, A. (2017). Simultaneous influence of pectin and xyloglucan on structure
888 and mechanical properties of bacterial cellulose composites. *Carbohydrate*
889 *Polymers*, *174*, 970–979. https://doi.org/10.1016/J.CARBPOL.2017.07.004
890 Velásquez-Cock, J., Ramírez, E., Betancourt, S., Putaux, J.-L., Osorio, M., Castro, C.,
891 … Zuluaga, R. (2014). Influence of the acid type in the production of chitosan
892 films reinforced with bacterial nanocellulose. *International Journal of Biological*
893 *Macromolecules*, *69*, 208–213. https://doi.org/10.1016/j.ijbiomac.2014.05.040
894 Vilela, C., Pinto, R. J. B., Coelho, J., Domingues, M. R. M., Daina, S., Sadocco, P., …
895 Freire, C. S. R. (2017). Bioactive chitosan/ellagic acid films with UV-light
896 protection for active food packaging. *Food Hydrocolloids*, *73*, 120–128.
897 https://doi.org/10.1016/j.foodhyd.2017.06.037
898 Wang, X., Guo, C., Hao, W., Ullah, N., Chen, L., Li, Z., & Feng, X. (2018).
899 Development and characterization of agar-based edible films reinforced with nano-
900 bacterial cellulose. *International Journal of Biological Macromolecules*, *118*, 722–
901 730. https://doi.org/10.1016/j.ijbiomac.2018.06.089

Wang, X., Xie, Y., Ge, H., Chen, L., Wang, J., Zhang, S., … Feng, X. (2018). Physical properties and antioxidant capacity of chitosan/epigallocatechin-3-gallate films reinforced with nano-bacterial cellulose. *Carbohydrate Polymers*, *179*, 207–220. https://doi.org/10.1016/J.CARBPOL.2017.09.087

Wexler, A. (1976). Vapor Pressure Equation for Water in Range 3 To 100 Degrees C. *Journal of Research of the National Bureau of Standards - A. Physics and Chemistry*, *80A*(3), 775–785. https://doi.org/10.6028/jres.075A.022

Yamada, Y., Yukphan, P., Lan Vu, H. T., Muramatsu, Y., Ochaikul, D., Tanasupawat, S., & Nakagawa, Y. (2012). Description of Komagataeibacter gen. nov., with proposals of new combinations (Acetobacteraceae). *The Journal of General and Applied Microbiology*, *58*(5), 397–404. https://doi.org/10.2323/jgam.58.397

Zhao, Y., Teixeira, J. S., Gänzle, M. M., & Saldaña, M. D. A. (2018). Development of antimicrobial films based on cassava starch, chitosan and gallic acid using subcritical water technology. *The Journal of Supercritical Fluids*, *137*, 101–110. https://doi.org/10.1016/J.SUPFLU.2018.03.010